J. Korea Asso. Radiat. Prot.
Vol. 28 No. 4 : 343~348(2003)

■論 文■

Performance of Gas Electron Multiplier (GEM) detector

S.H. Han* · B.S. Moon* · Y.K. Kim* · C.E. Chung* · H.D. Kang** and H.S. Cho***

*Korea Atomic Energy Research Institute,
**Department of Physics, Kyungpook National University
***Department of Medical Engineering, Research Institute of Biomedical Engineering, Yonsei University

(AOCRP-1 ORAL 발표, 2003년 12월 8일 채택)

Abstract - We have investigated in detail the operating properties of Gas Electron Multiplier (GEM) detectors with a double conical and a cylindrical structure in a wide range of external fields and GEM voltages. With the double conical GEM, the gain gradually increased with time by 10%; whereas this surface charging was eliminated with the cylindrical GEM. Effective gains above 1000 were easily observed over a wide range of collection field strengths in a gas mixture of Ar/CO_2(70/30). The transparency and electron collection efficiency were found to depend on the ratio of external field and the applied GEM voltage; the mutual influence of both drift and collection fields was found to be trivial

Key words : GEM, transparency, collection efficiency, effective gain

INTRODUCTION

The development of microstructure gas detectors is under very active research, many innovative devices having been proved capable of a more reliable and powerful operation in high intensity radiation environments. The recently introduced Gas Electron Multiplier (GEM)[1] has proven to be very promising and robust against spark damage compared with other existing microstructure devices such as Micro-Strip Gas Chamber (MSGC) and Micro-Gap Chamber (MGC)[2-8]. Since the amplification stage of GEM is separated from the charge collection structure and only electrons are detected at the collection electrode, the collection signal is very fast and safe without propagation of a discharge to the collection electrode[9,10].

The double conical GEM consists of a thin insulating 50-μm-tick Kapton foil, which is metal plated on both sides (5-μm-thick copper) and which is perforated by a compact array of small open holes that act as multiplication channels (see Fig. 1(left)). The GEM was manufactured at CERN with a hole pitch of 100 μm, a hole diameter of 60 μm in the metal layer, and an active area of 10 × 10 cm^2. A double conical GEM produced by chemical etching has a polyimide cone protruding into the channel. The laser machined cylindrical GEM, however, provides nearly vertical sidewalls. The insulator thickness of the cylindrical GEM, with a hole pitch of 400 μm and a hole diameter of 150 μm, is 125 μm, more than twice as thick as the double conical GEM

Under application of a suitable potential difference between the GEM electrodes with a GEM foil inserted between drift and collection electrode planes, a strong dipole field is built up in the holes focusing the drift field lines. Electrons produced by ionization in the drift region are

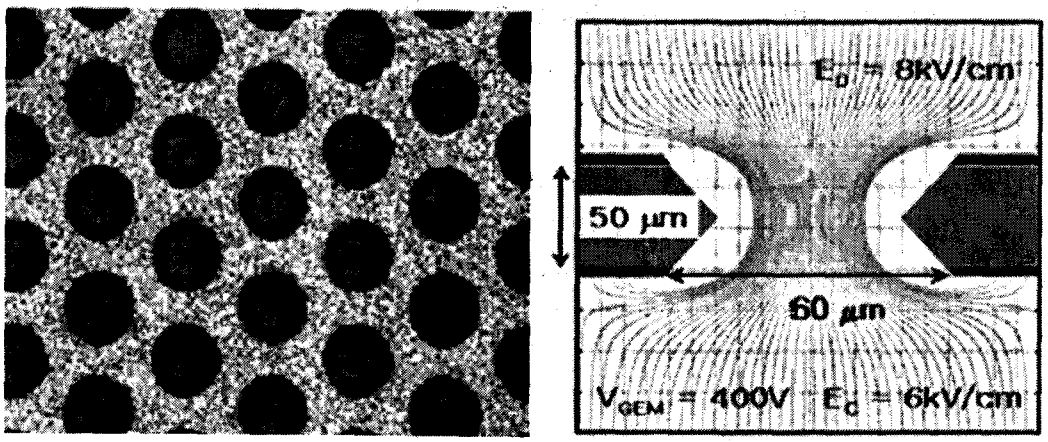

Fig. 1. (left) Photo of a double conical GEM and (right) electric field map: some field lines terminate on the bottom GEM electrode.

accelerated into the holes where they are multiplied by the high electric field and transferred to the collection electrode, thus inducing a signal current. However, a fraction of the primary electrons from the drift region may reach the top GEM electrode, and a substantial fraction of the electrons released within the GEM channels become trapped by the bottom GEM electrode; this fraction strongly depends on the external electric fields[11]. For a better understanding of the GEM operation, Fig. 1(right) shows an electric field map computed using MAXWELL[12] and GARFIELD[13].

EXPERIMENTAL SETUP

The test assembly (see Fig. 2) used to demonstrate the operation of the GEM was installed in a stainless-steel box with a Be window. The drift electrode, which is made of an aluminized mylar sheet, is located 3 mm above the GEM and is negatively biased relative to it, thus creating a drift field, E_D, for the electrons which are ionized by absorption of X-rays in the upper drift region (or conversion region). On approaching the GEM hole from the drift region, electrons begin to multiply in an avalanche, increasing exponentially along the channel, and are collected on the bottom GEM and collection

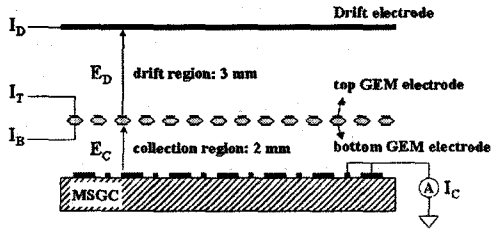

Fig. 2. Schematic of the combined detector with the GEM and MSGC.

electrodes. The gap between the bottom GEM electrode and the collection electrode, which is referred to as the collection region, is 2 mm, and E_C indicates the collection field, the electric field in the collection region. A MSGC (micro-strip gas chamber) with 95-μm-wide cathode strips (200-μm pitch) was used as the collection electrode; groups of MSGC anodes and cathodes were connected together and grounded through a picoammeter. The MSGC was not operated, except during the measurement of the X-ray flux. The currents flowing into all four electrodes were monitored independently using CAEN N471A high-voltage power supplies and a picoammeter. High-purity argon (99.9999 % pure) and CO_2 (99.99 % pure) in a volume proportion of 70/30 were used in all measurements. The detector was irradiated with a 5.9-keV ^{55}Fe X-ray source with a typical detected flux corresponding to 580 $mm^{-2}s^{-1}$.

The effective gain was determined by measuring the electron signal current on the collection electrode, Ic, and the count rate, R, for the X-ray spectrum separately; the effective gain G is given by $I_C/(RNe)$, where e and N denote the electron charge and the known number of electron-ion pairs per conversion (~220 for 5.9 keV), respectively. Owing to electron charge losses in the bottom GEM electrode, the absolute gas gain is generally larger by a field- and geometry- dependent factor.

RESULTS AND DISCUSSION

Gas Multiplication

The primary interest of gaseous detectors is to achieve safely high gains. In regard to GEM, this can be realized by increasing the field density in the GEM channels. The field strength depends on geometry, increasing with the reduction of the hole diameter and the insulator thickness as well as with the potential difference between the two GEM electrodes. Fig. 3 shows the electric field strength along a vertical line in the central region of GEM hole, calculated using MAXWELL electric field simulator. With drift and collection fields of 1 kV/cm and 6 kV/cm respectively, the maximum field strength of both GEMS in the center of the hole exceeds $2x10^6$ V/m even at low GEM voltages; this is sufficient to induce an avalanche multiplication for electrons drifting through the GEM. The double conical GEM operated at lower applied voltages due to the increase of electric field strength in the GEM hole by the smaller holes, while the maximum gains are similar in both GEMs because of the longer amplification path of the cylindrical GEM as shown in Fig. 4.

In the double conical GEM structure, the protruding insulator into the multiplication channels introduces the possibility of charge deposition on the insulating surface. No external drift field lines entering the amplification holes end on the insulating Kapton surface, but collision diffusion and processes induced by photon could induce charge collection on the insulator in point of fact. The charge deposited in the GEM hole pushes out field lines previous ending at the insulating surface. The result is the increase of the field strength in the avalanche region of the GEM hole and so an initial gain increase with time. Fig. 5 shows the time dependence of gain for the double conical GEM and the cylindrical GEM under a X-ray rate of 3x10 $mm^{-2}s^{-1}$ with effective gain of 200. A double conical GEM had a gain increase of about 10% during the first hour of operation. A cylindrical GEM had a no noticeable gain shift during the operation due to

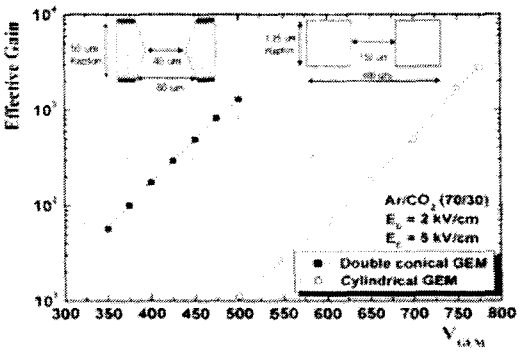

Fig. 4. Dependence of effective gain as a function of GEM voltage for the double conical and cylindrical GEMs.

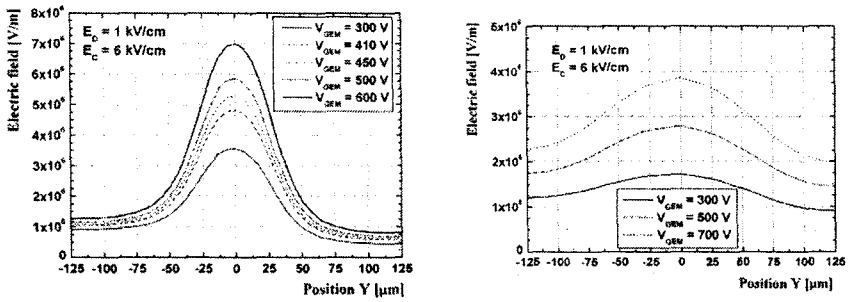

Fig. 3. Electric field strength in the holes of (left) double conical and (right) cylindrical GEMs.

no protrusions of the insulator. This gain increase can be eliminated making the insulating surface slightly conductive by a doped amorphous silicon or Diamond-Like carbon(DLC) coating.

Figure. 6(left) shows the effective GEM gain as a function of the potential difference between the top and the bottom GEM electrodes, V_{GEM}, for different collection fields at a fixed drift field of 1 kV/cm. The maximum effective gain was about 3.5×10^3 for a collection field of 6 kV/cm and a GEM voltage of 510 V. Lower operation voltages, of around 400 V, are obtained at high collection fields, and the maximum attainable gains remain relatively constant for collection field above 3 kV/cm. Effective gas gains above 10^3 can be attained over a wide range of collection field strengths, providing around 2 times greater gain at the same GEM voltage than has been reported in earlier papers[11,14], due to the smaller GEM holes and thus the higher electric field in the multiplication GEM channels.

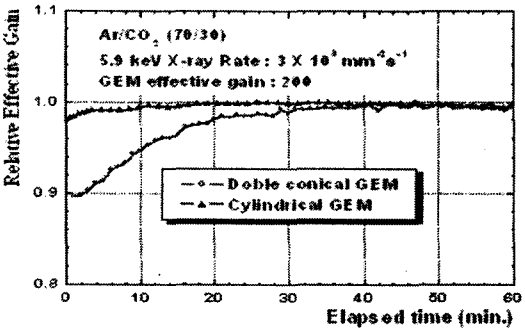

Fig. 5. Time dependent gain shift, due to charge deposit on the insulating surface within the amplification holes.

To cover large active areas, it is of high importance that the response of the whole detector surface is homogeneous. The uniformity of gas gain of the detector has been measured by displacing the collimated source with a diameter of 1 mm across the active area; the normalized gain of the chamber is very constant, with a deviation of 2%, as shown in Fig. 6(right). Since the gain has a strong dependence on the hole size and the thickness of the insulator, this shows the high precision of the manufacturing which was reached.

Electron Collection Efficiency and Transparency

We measured the collection efficiency, defined as the fractional collection current, I_C/I_{TOT} ($I_{TOT} = I_B + I_C$), as a function of the collection field for drift fields of 2 kV/cm and 5 kV/cm at a GEM voltage of 410 V. The collection efficiency increased in a nearly linear fashion with the collection field up to 90% at E_C = 8 kV/cm, but was essentially independent of the drift field strength [14, 15], as shown in Fig. 7(left). From the collection efficiency measurement, it was apparent that a considerable fraction of the electron charge in the avalanche flows into the bottom GEM electrode; for a collection field of 1 kV/cm, this fraction was above 90%. The collection efficiency is practically independent of the drift field for the two values of the collection field used herein, as shown in Fig. 7(right). As mentioned above, the collection efficiency increases in a nearly linear fashion with the collection field, reaching

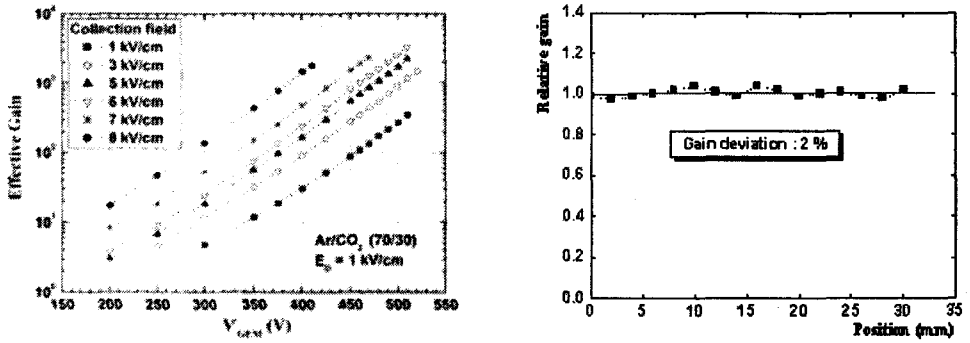

Fig. 6. (left) Effective gain as a function of GEM voltage for different collection electric fields and (right) gain uniformity. Lower GEM operation voltages of around 400 V were obtained at high values of the collection field. The maximum effective gain was about 3.5×10^3 for a collection field of 6 kV/cm and a GEM voltage of 510 V.

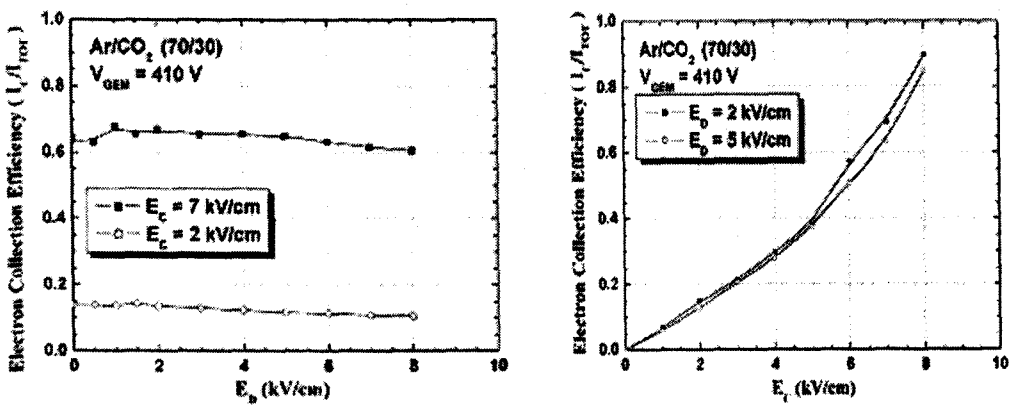

Fig. 7. Electron collection efficiency with respect to (left) collection field and (right) drift field.

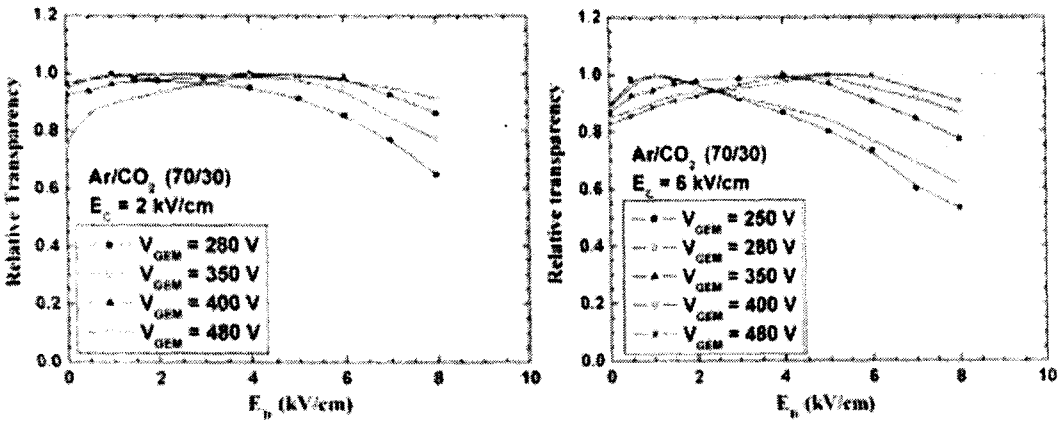

Fig. 8. Relative transparency as a function of drift field for several GEM voltages and a collection field of (left) 2 kV/cm and (right) 6 kV/cm.

approximately 15 % and 65 % at Ec = 2 kV/cm and 7 kV/cm, respectively.

Another crucial parameter that affects the collection efficiency is transparency, which is defined as the fraction of primary electrons passing through the GEM multiplying holes. The value of this fraction depends both on the ratio of the open area to the total GEM area, the optical transparency, and on the proportion of field lines passing through the GEM holes, the electrical transparency. The electrical transparency can be adjusted by altering the drift field strength relative to that in the holes. Figures 8(a) and (b) show the observed relative transparency defined as the collection current normalized to its maximal value, $I_C/I_{C,max}$. At a high drift field, some electric field lines terminate on the GEM top electrode, thus reducing the transfer of electrons into the channels. At very low drift fields, on the other hand, an increase in diffusion and electron-ion recombination plays a role in the loss of electrons. For a given GEM geometry, the drift field range of efficient electron collection showing a plateau increases with the applied GEM voltage, but is nearly independent of the collection field, a behavior that has been reported in Refs. 16 and 17. The region of the drift field where the GEM is completely transparent, indicative of a full primary electron collection from the drift gap, extends to around 8 kV/cm at high GEM voltages of 400 V and 480 V.

RESULTS AND DISCUSSION

The dependences of gas multiplication and electron transfer on the external field and the GEM voltages were examined with double conical and cylindrical GEMs. Low GEM operation voltages are possible because of the gain enhancement caused by the narrower holes. The presence of an insulator close to the multiplication channels of GEM introduces the possibility of charge deposition on the insulating surface, resulting in an increase of the field strength within the hole and therefore a moderate gain shift. With the double conical GEM, the gain gradually increased with time by 10%; whereas this surface charging was eliminated with the cylindrical GEM.

The collection efficiency increased in a nearly linear fashion with the collection field, reaching approximately 15% and 65% at Ec = 2 kV/cm and 7 kV/cm, respectively but the strength of drift field had a negligible influence on it. The extension of the region of efficient electron collection from the drift gap depends on the GEM voltage, but is nearly independent of the collection field.

REFERENCES

1. F. Sauli, Nucl. Instr. Meth. A 386, 531 (1997)
2. R. Bouclier, M. Capeáns, W. Dominik, M. Hoch, J-C. Labbé, G. Million, L. Ropelewski, F. Sauli, and A. Sharma, IEEE Trans. Nucl. Sci. NS-44, 646 (1997)
3. R. Bouclier, W. Dominik, M. Hoch, J-C. Labbé, G. Million, L. Ropelewski, F. Sauli, A. Sharma, and G. Manzin, Nucl. Instr. Meth. A 396, 50 (1997)
4. S. Bachmann, S. Kappler, B. Ketzer, T. Müller, L. Ropelewski, F. Sauli, and E. Schulte, Proceedings of the Vienna Conference on Instrumentation, Feb (2001)
5. J. Benlloch, A. Bressan, C. Büttner, M. Capeáns, M. Gruwé, M. Hoch, J-C. Labbé, A. Placci, L. Ropelewski, F. Sauli, A. Sharma, and R. Veenhof, IEEE Trans. Nucl. Sci. NS-45, 234 (1998)
6. Hyosung Cho, Sanghyo Han, and Heedong Kang, J. Korean Phys. Soc. 39, 230 (2001); F. A. F. Fraga, S. T. G. Fetal, R. Ferreira Marques, and A. J. P. L. Policarpo, Nucl. Instr. Meth. A 442, 417 (2000)
7. E. K. E. Gerndt, B. A. Knapp, J. Miyamoto, I. P. J. Shipsey and Q. Zhang, Nucl. Instr. Meth. A 422, 282 (1999)
8. F. A. F. Fraga L. M. S Margato, S. T. G. Fetal, M. M. F. R. Fraga, R. Ferreira-Marques, A. J. P. L. Policarpo, B. Guerard, A. Oed, G. Manzin, and T. van Vuure, CCD readout of GEM-based neutron sources , paper presented at the Vienna Conf. on Instrumentation, Feb. 19-23 (2001)
9. F. Sauli, Nucl. Instr. Meth. A 419, 189 (1998)
10. A. Bressan, R. de Oliveira, A. Gandi, J-C. Labbé, L. Ropelewski, F. Sauli, D. Mörmann, T. Müller, and H. J. Simonis, Nucl. Instr. Meth. A 425, 254 (1999)
11. J. Benlloch, A. Bressan, M. Capeans, M. Gruwé, M. Hoch, J-C. Labbé, A. Placci, L. Ropelewski, and F. Sauli, Nucl. Instr. Meth. A 419, 410 (1998)
12. MAXWELL electric field simulator, Ansoft Co., Pittsburg, PA, USA.
13. R. Veenhof, Nucl. Instr. Meth. A 419, 726 (1998)
14. S. Bachmann, A. Bressan, L. Ropelewski, F. Sauli, A. Sharma, and D. Mörmann, Nucl. Instr. Meth. A 438, 376 (1999)
15. A. Bressan, A. Buzulutskov, L. Ropelewski, F. Sauli, and L. Shekhtman, Nucl. Instr. Meth. A 423, 119 (1999)
16. R. Bouclier, W. Dominik, M. Hoch, J-C. Labbé, G. Million, L. Ropelewski, F. Sauli, A. Sharma, and G. Manzin, Nucl. Instr. Meth. A 396, 50 (1997)
17. R. Bellazzini, A. Brez, G. Gariano, L. Latronico, N. Lumb, G. Spandre, M. M. Massai, R. Raffo, and M. A. Spezziga, Nucl. Instr. Meth. A 419, 429 (1998)